Journal of Power Sources 194 (2009) 618–624

Contents lists available at ScienceDirect

Journal of Power Sources

journal homepage: www.elsevier.com/locate/jpowsour

Mass spectroscopy for the anode gas layer in a semi-passive direct methanol fuel cell using porous carbon plate
Part II. Relationship between the reaction products and the methanol and water vapor pressures

M. Shahbudin Masdar, Takuya Tsujiguchi, Nobuyoshi Nakagawa*

Department of Chemical and Environmental Engineering, Gunma University, 1-5-1 Tenjin-cho, Kiryu, Gunma 376-8515, Japan

ARTICLE INFO

Article history:
Received 14 April 2009
Received in revised form 14 July 2009
Accepted 14 July 2009
Available online 22 July 2009

Keywords:
Semi-passive DMFC
Intermediate products
Methanol oxidation
Production rate
Product distribution

ABSTRACT

Subsequent to Part I, in situ mass spectrometry using a capillary probe was conducted in order to evaluate the gas condition of the anode gas layer of a semi-passive direct methanol fuel cell (DMFC) employing a porous carbon plate (PCP). Different types of PCPs were used for the DMFC, and the production of intermediates besides CO_2, i.e., methylformate ($HCOOCH_3$), formaldehyde (HCHO) and formic acid (HCOOH), were investigated. The profiles of the vapor pressures of these products were related to the vapor pressure of methanol and water in the gas layer. The production rate of each intermediate was formulated as a power function of the methanol and water vapor pressure ratio, P_{CH_3OH}/P_{H_2O}, with the power factors of 2.07, 0.47 and −0.57 for methylformate, formaldehyde and formic acid, respectively. Based on these equations of the production rates, the product distribution could be quantitatively estimated.

1. Introduction

Direct methanol fuel cells (DMFCs) based on a polymer electrolyte membrane have received much attention as the leading power source candidate for mobile and portable applications because of their high energy density and energy-conversion efficiency [1–5]. However, the commercialization of the DMFC has been still hindered due to several technological problems [6–8] including methanol crossover (MCO) through the polymer membrane, low electro-catalytic activity of the methanol oxidation on the anode [9] and severe cathode flooding [10]. As a result of the MCO, the DMFC has usually been operated with a methanol solution at low concentration, i.e., 1–3 M [11,12] under active conditions and 5 M [13–15] under passive conditions. It is important to use a high concentration of methanol in DMFC for achieving a high energy density.

Recently, we have demonstrated that a DMFC with a novel electrode structure employing a porous carbon plate (PCP) at the anode could efficiently be operated using methanol at very high concentrations up to 100% [16–20]. The porous plate significantly controlled the MCO through the MEA. At the anode, a gas layer dominated by CO_2 is formed on the anode surface, resulting in methanol being transported to the anode as a vapor. Hence, the gas layer atmosphere is directly related to the electrode performance and also the MCO. In a previous paper, Part I, we clarified the relationship between the current density and vapor pressures of methanol and water in the DMFC with PCP by applying in situ mass spectroscopy using a capillary probe, and showed that the actual methanol activity in the gas layer is similar to that of methanol solution at a low concentration used in the conventional type of passive DMFCs.

In this study, we focused on the production of the intermediates, i.e., methylformate ($HCOOCH_3$), formaldehyde (HCHO) and formic acid (HCOOH), at the anode using mass spectroscopy. The production of the intermediates reduces the energy-conversion efficiency of the DMFC and also some of the products are harmful to human health [23]. Although we have reported the production rates of the intermediates in the DMFC with PCP [20], the production rate was correlated with the MCO as a function related to the methanol activity at the anode because we did not have a proper technique for measurement of the gas composition in the gas layer.

With respect to the products from the electrochemical oxidation of methanol with water, carbon dioxide is the main product, while methylformate, formaldehyde, formic acid, methylal ($CH_2(OCH_3)_2$) and carbon monoxide (CO) are commonly detected as minor products [20–31]. The product distribution and the production rates were affected by the oxidation conditions such as methanol feed either as a liquid [21] or vapor [30], the methanol/water mole ratio [25], MCO [20], temperature, current density and electrolyte [23,24] as well as the catalyst morphology [24,26]. At a high methanol activ-

* Corresponding author. Tel.: +81 277 30 1458; fax: +81 277 30 1457.
E-mail address: nakagawa@bce.gunma-u.ac.jp (N. Nakagawa).

0378-7753/$ – see front matter © 2009 Elsevier B.V. All rights reserved.
doi:10.1016/j.jpowsour.2009.07.026

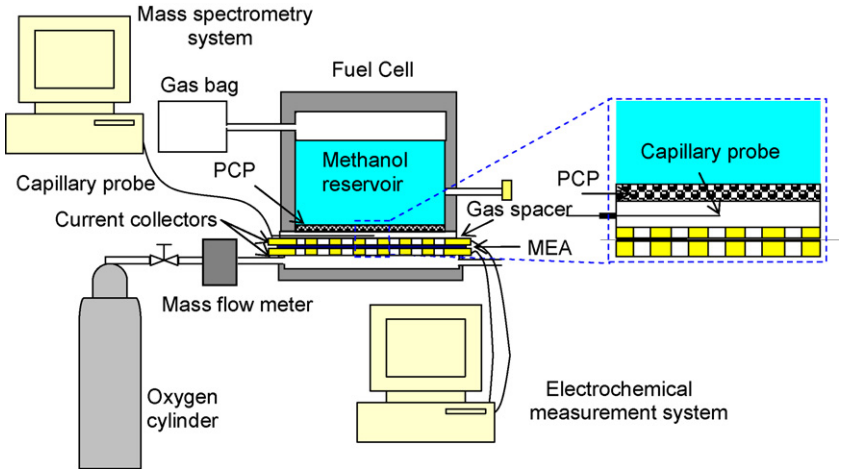

Fig. 1. Experimental setup that combined a passive DMFC with PCP and a mass spectrometer.

ity, i.e., high methanol partial pressure or high methanol/water ratio, methylformate and sometimes methylal have a tendency to be significantly produced [22,24,27] and the distribution of these products under some conditions could be achieved up to 80% besides CO_2 [22]. However, at a low methanol activity, i.e., when excess water is present, these products become negligible and formaldehyde and formic acid were the predominant products besides CO_2 and the formaldehyde was sometimes obtained up to about a 75% distribution [27]. Although almost all of these references were not directly related to an actual DMFC operation, the results reported therein raised the concern about the intermediate formation during the methanol oxidation [21–29]. Only a few papers analyzed the intermediate products during a real time DMFC operation [20,30,31]. Otherwise, for the all references [20–31], they did not explain the quantitative relationship between the production rate of intermediate products or their distribution and the methanol oxidation conditions, i.e., methanol/water mole ratio, current density, temperature, etc. This relationship is important and has an advantage to predict the production rate or product distributions for different methanol oxidation conditions.

In this study, by using the mass-spectrometry technique, the gas composition in the gas layer of the DMFC with PCP was directly measured during power generation, and the relationships between the production rates and the gas composition were qualitatively evaluated for the intermediate products besides CO_2. The gas composition was varied by applying different PCPs with different pore structures and by using different methanol concentrations. The product distribution rate besides CO_2 was calculated as a function of the ratio of the methanol and water partial pressures, P_{CH_3OH}/P_{H_2O}, based on the production rates of each intermediate product.

2. Experimental

2.1. Semi-passive DMFC with PCP

Fig. 1 shows the semi-passive DMFC with PCP and the experimental setup for the analysis of the gas composition in the anode gas layer used in this study.

Four types of PCPs supplied from Mitsubishi Pencil Co. Ltd., were used in the DMFC operation. The analyzed pore structures for the different PCPs are shown in Table 1. The perm-porosimeter (Porous Materials Inc.) was used for the measurement of the properties of PCP, i.e., resistivity to a fluid flow through the PCP and the pore structure like pore diameter. Darcy constant's, k ($=F\mu L/(A\Delta P)$, where, F, volumetric flow rate of the fluid; μ viscosity of the fluid; L, thickness of the porous plate; A, surface area; ΔP, pressure drop through the plate), for air flow was obtained, and the bubble point pressure was also measured using Galwick solution with surface tension 15.7 dyne cm^{-1} for the different PCP. The resistance, R ($=L/k$), shown in the table was calculated based on the Darcy constant, k, and the thickness, L, and was used as an indicator to show the resistance of the methanol transport through the PCP.

The MEA with a 5 cm^2 area, in which Pt and Pt-Ru black were used as the catalyst for the cathode and anode, respectively, was prepared in the same manner as described in our previous papers [16–20]. The catalyst loading was 10 mg cm^{-2} for Pt and 12 mg cm^{-2} for Pt-Ru while Nafion 112 was used as the membrane electrolyte.

The semi-passive DMFC employing PCP, shown in Fig. 1, was slightly modified for the gas sampling compared with our previous DMFC [16–20] by putting a gas spacer, with a 3.0 mm thickness, between the PCP and the anode current collector. Therefore, the space for the anode gas layer was increased by 3.0 mm when compared to the original cell structure. By putting the gas spacer, resistance for the mass transport would little bit increased and slightly affected the cell performance [17] compared to that of the original. The capillary probe, with a 30 μm inner diameter, from the mass spectrometer was inserted through a hole in the spacer and placed in the middle of the gas layer space as shown in Fig. 1. The cathode was covered with a thin chamber, and oxygen from a cylinder was flowed through the chamber in order to collect the exhaust gas.

The DMFC with the PCP was operated by injecting a methanol solution with a certain concentration into the reservoir and by feeding oxygen to the cathode at 35 ml min^{-1} under ambient conditions. Power generation was conducted at a certain cell voltage for 4 h. The electrochemical performance of the cell was measured using an

Table 1
PCPs properties.

PCP	Thickness (mm)	Bubble point pressure (kPa)	Average pore diameter (μm)	Darcy constant, k (m^2)	Resistance, R (m^{-1})
Y1	1.0	7.0	1.9	4.2E−14	2.4E+10
Y1.5	1.5	2.0	10.6	3.1E−13	4.9E+09
Y2A	2.0	4.7	1.6	2.5E−13	8.1E+09
Y2B	2.0	1.1	17.3	8.7E−13	2.3E+09

HZ3000 electrochemical measurement system (Hokuto Co. Ltd.).

On the other hand, in situ mass spectroscopy with the capillary probe was carried out to evaluate the gas composition in the anode gas layer during cell operation. The calibration for the conversion of the ion current intensity into vapor pressure was conducted by determining the sensitivity factor for each component by measuring the vapor pressure of the pure component under certain conditions or a standard gas with a known composition. The vapor pressure or partial pressure of each component was then calculated from its contribution to the ion intensity for the main mass fragment of the component using the sensitive factor obtained by the calibration. A detailed explanation of the DMFC operation and the gas analysis has been described in our previous paper, Part I.

2.2. Evaluation of the production rate of the intermediate products

During the operation, the gas produced from the anode was collected in a gas bag that was connected to the outlet tube as shown in Fig. 1. After 4 h of power generation at a constant cell voltage, the amount and the composition of the solution in the reservoir was analyzed by using the gas chromatography and the gaseous products collected in the bags were analyzed using both of the gas chromatography and the mass spectrometry. Then, the production rates of each component were calculated as the average production rate for the 4 h operation. For the quantitative analysis of the products, a gas chromatography with columns of Porapack-T/PEG6000; for both gaseous products and solution in the reservoir; and a UV technique (Nash method [32] for formaldehyde); only for solution; were used.

3. Results and discussion

3.1. Formation of the intermediate products

3.1.1. Intermediate products detected by mass spectrometry

Under all conditions of this experiment, the gas composition in the anode gas layer was mainly dominated by CO_2 followed by methanol and water, as already described in the previous paper, Part I. As a minor product, the mass spectral analysis showed a minor peak at $m/z = 60$, for methylformate, $[HCOOCH_3]^+$, in the range $18 \leq m/z \leq 75$ of this measurement. We quantitatively analyzed the other mass fragments detected in this range, for example $m/z = 29$, based on the relative abundance data [33] for the possible species from the methanol oxidation, and confirmed that methylformate, formic acid and formaldehyde were formed as minor products during this experiment.

The contribution in the ion intensity of each component by a certain mass fragment was separated using the relative abundance data and the ion intensities for the different mass fragments. The vapor pressure or partial pressure of each component was then calculated from the contribution in the ion intensity for the main mass fragment of the component using the sensitive factor obtained by the calibration.

3.1.2. Profile of the intermediate products during the DMFC operation

Figs. 2–6 show the profiles of the intermediate products versus the operation time of the DMFC with the porous carbon plate, Y2B. Each figure was obtained at different methanol concentration in the reservoir, and the partial pressures of methanol, P_{CH_3OH}, and water, P_{H_2O}, are plotted in (a) and that of the methylformate, formic acid, and formaldehyde are shown in (b) in the figure. It was clearly shown in the figures that P_{CH_3OH} and P_{H_2O} depended on the methanol concentration in the reservoir, and P_{CH_3OH} and P_{H_2O} increased with the increasing methanol concentration. At low

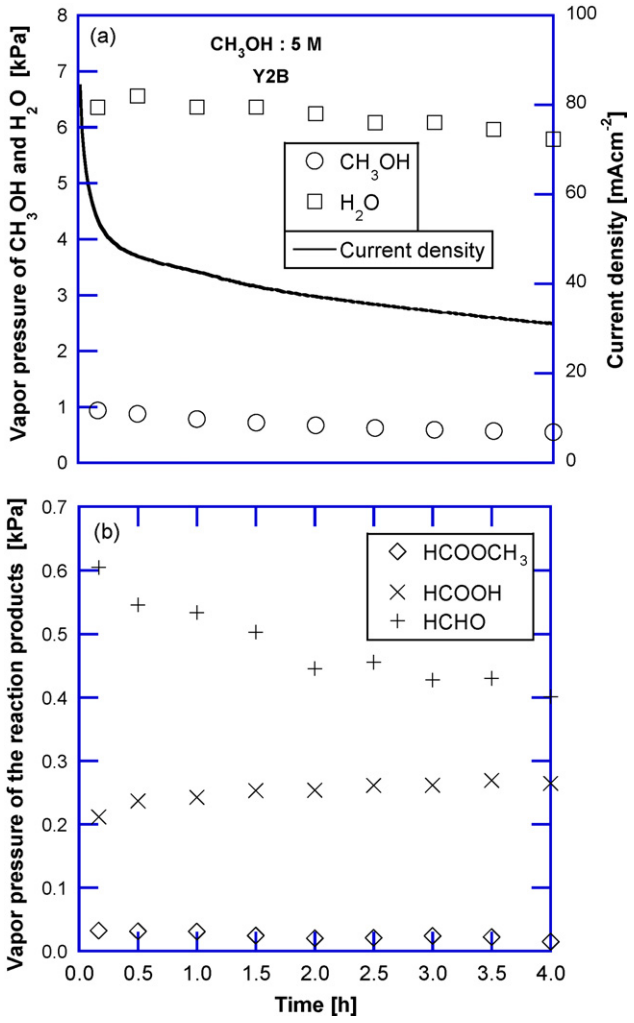

Fig. 2. Profiles of (a); vapor pressure of methanol, P_{CH_3OH}, and water, P_{H_2O}, and (b); the intermediate product in the anode gas layer with time at 5 M.

methanol concentrations, 5 M and 12 M shown in Figs. 2 and 3, respectively, P_{CH_3OH} and P_{H_2O} were nearly constant during the cell operation, while at high methanol concentrations, 16 M, 22 M and 24.7 M shown in Fig. 4, Fig. 5 and Fig. 6, respectively, P_{CH_3OH} and P_{H_2O} changed with time. P_{CH_3OH} decreased with time and this could be related to the large consumption of methanol at the anode based on the high current densities. In case of 5 M and 12 M, Figs. 2 and 3, the high current density at the initial would be related to the initial methanol that has been accumulated in the PCP under the open circuit conditions as mentioned in our previous paper, Part I and reports [18,19]. In case of 16 M, Fig. 4, the accumulation of methanol in the PCP might be low at the beginning of the operation. Whereas, for all the cases, P_{H_2O} initially increased with time, but thereafter, it became nearly constant. The initial increase in P_{H_2O} may be related to water back diffusion from the cathode to the anode when then became constant when a steady state current density was reached. The profiles of these P_{CH_3OH} and P_{H_2O} were also influenced by the partial pressure of CO_2 which was the main product of the anode reaction as discussed in our previous paper, Part I.

Vapor pressures of the intermediates were almost one order of magnitude lower than that of methanol and water as shown in (b) of Figs. 2–6. Among the vapor pressures of the three intermediate components, formaldehyde was predominant followed by formic acid and then methylformate when the P_{CH_3OH} was lower than 4 kPa as shown in Figs. 2 and 3. When P_{CH_3OH} was between

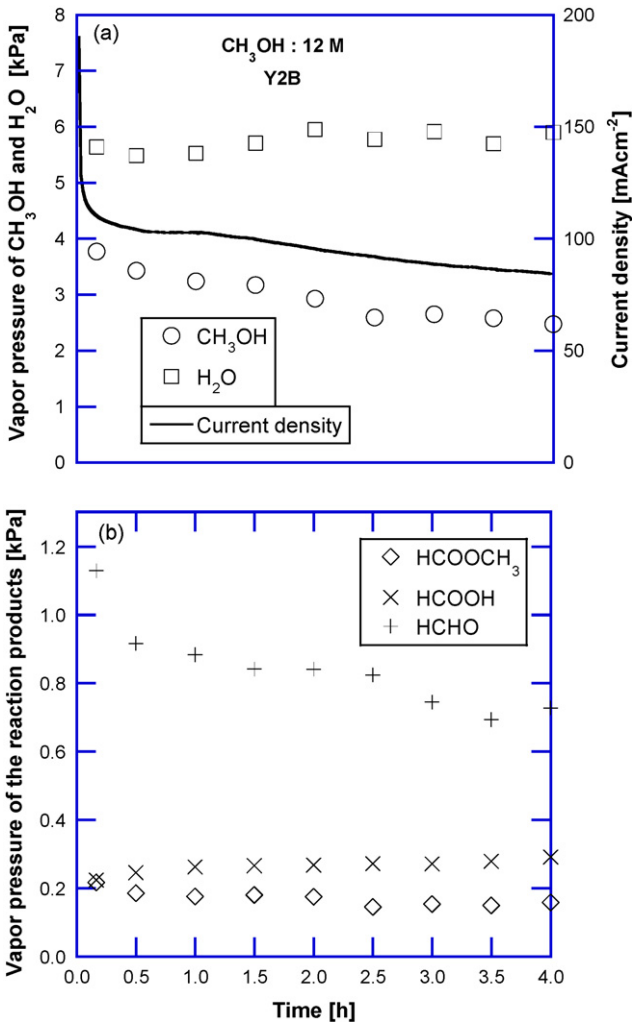

Fig. 3. Profiles of (a); vapor pressure of methanol, P_{CH_3OH}, and water, P_{H_2O}, and (b); the intermediate product in the anode gas layer with time at 12 M.

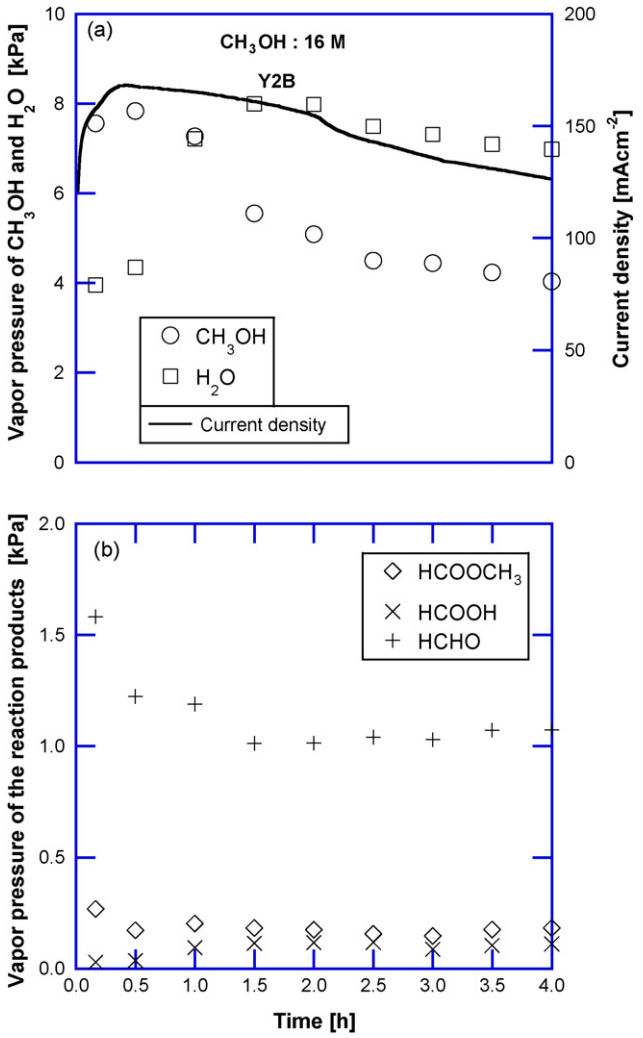

Fig. 4. Profiles of (a); vapor pressure of methanol, P_{CH_3OH}, and water, P_{H_2O}, and (b); the intermediate product in the anode gas layer with time at 16 M.

4 kPa and 8 kPa, formaldehyde was still predominant, but it was followed by methylformate and then formic acid as shown in Fig. 4. The vapor pressure of methylformate was predominant when $P_{CH_3OH} > 10$ kPa as shown in Figs. 5 and 6. These results indicate a strong correlation between the vapor pressure of methylformate and that of methanol. However, the vapor pressure of formic acid was only slightly affected by that of methanol and was in the range of 0.1–0.3 kPa in all experiments.

The vapor pressure profiles of the intermediate products must be related to the reaction mechanism of the methanol oxidation. For the methanol oxidation steps including formaldehyde, formic acid and methylformate as the intermediates, the following mechanism was considered on the basis of previous studies [20–31].

$$CH_3OH \rightarrow HCHO + 2H^+ + 2e^- \quad (1)$$

$$CH_3OH + H_2O \rightarrow HCOOH + 4H^+ + 4e^- \quad (2)$$

$$CH_3OH + HCOOH \leftrightarrow HCOOCH_3 + H_2O \quad (3)$$

$$HCOOH \rightarrow CO_2 + 2H^+ + 2e^- \quad (4)$$

As shown in Eqs. (1)–(4), the formation of each product would be related to each other.

Fig. 7 shows the relationship between the P_{CH_3OH} and vapor pressures of the other components in the anode gas layer by summarizing the data at 2 h during the measurement displayed in Figs. 2–6 including some additional data obtained at different methanol concentrations. This figure clearly shows a strong linear dependency of the vapor pressure of methylformate on P_{CH_3OH}, while that of formic acid has no dependency. The vapor pressure of water, one of the reactants in the oxidation reaction, increased with an increase in P_{CH_3OH}, suggesting that P_{H_2O} was also related to the formation of the intermediate products.

3.2. Production rates as a function of P_{CH_3OH}/P_{H_2O}

The production rate of the intermediate that was obtained by the analysis of the remaining solution in the reservoir, and it was correlated with the methanol and water vapor pressure ratio, P_{CH_3OH}/P_{H_2O}, at 2 h, while no products other than CO_2 were detected in the gas bag connected to the reservoir by using both of the gas chromatography and the mass spectrometry. We have confirmed that the methanol and water vapor pressure ratio was the most appropriate variable for formulating the production rate of each intermediate from some trials to determine the formation of variables using the methanol and/or water vapor pressure. Savinell and co-workers [30] have also shown that the formation of the intermediate products increased with the increasing mole ratio of methanol to water.

Figs. 8–10 show the relationship between the production rate of the each intermediate and P_{CH_3OH}/P_{H_2O} at 2 h, methylformate, formaldehyde and formic acid in Figs. 8–10, respectively. In these

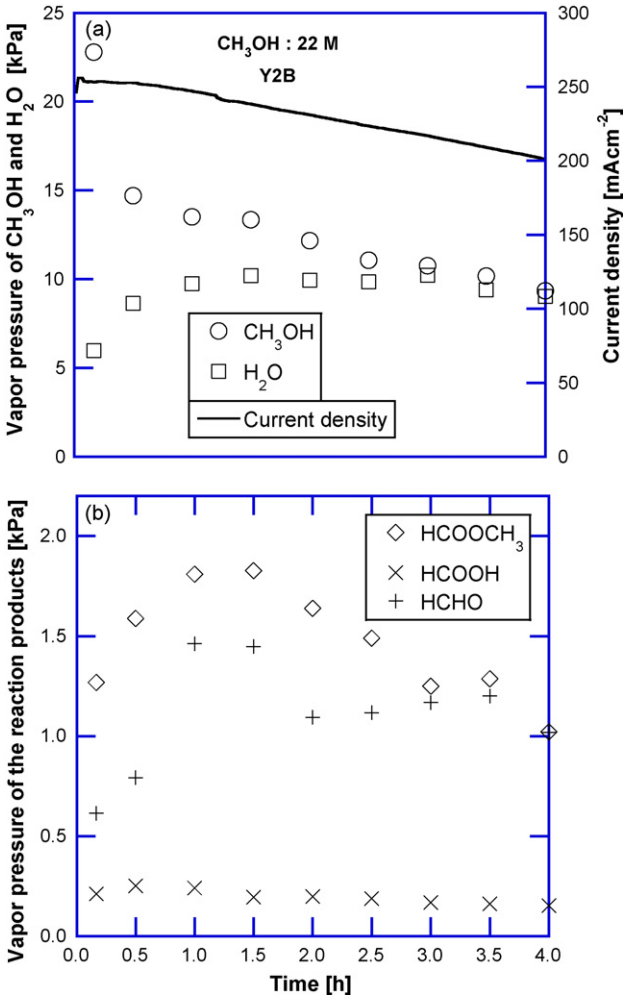

Fig. 5. Profiles of (a); vapor pressure of methanol, P_{CH_3OH}, and water, P_{H_2O}, and (b); the intermediate product in the anode gas layer with time at 22 M.

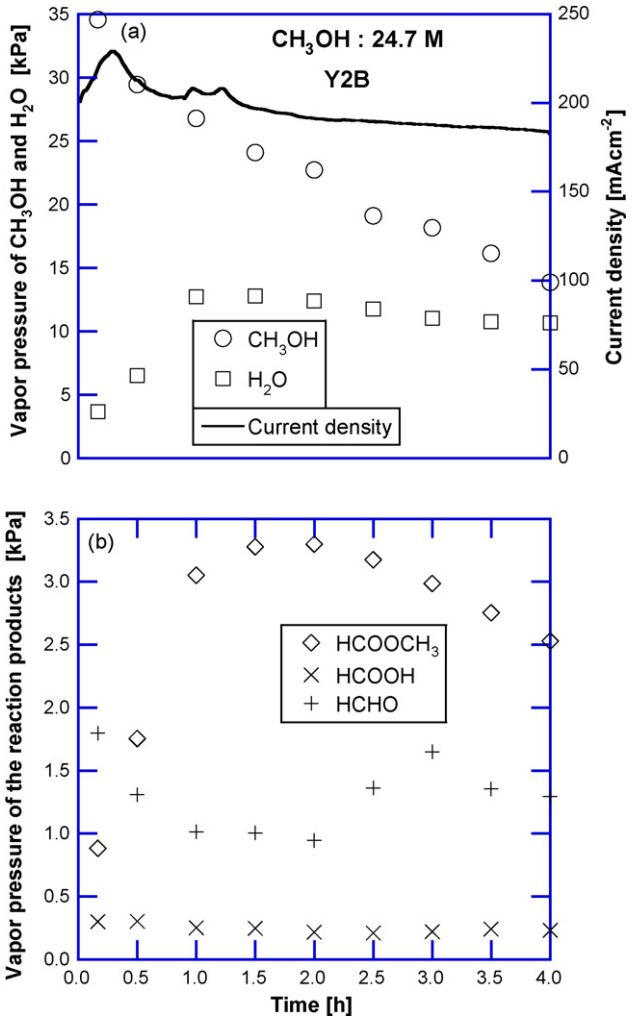

Fig. 6. Profiles of (a); vapor pressure of methanol, P_{CH_3OH}, and water, P_{H_2O}, and (b); the intermediate product in the anode gas layer with time at 24.7 M.

figures, the production rate of the intermediates and the vapor pressure, P_{CH_3OH} and P_{H_2O}, were calculated as an average for the 4 h operation of the experiment. Also, all the data obtained from the experiments using the different types of PCPs, i.e., Y1, Y1.5 Y2A and Y2B, and different methanol concentrations, were plotted. One can see the very good correlations between the production rate of the intermediates and the methanol and water vapor pressure ratio in each figure. The ratio of the vapor pressure, P_{CH_3OH}/P_{H_2O}, not the pressures themselves, as the variable for the production rates suggests that the production rate of the intermediates, explained by Eqs. (1)–(4), occurs through a reaction step by the strongly adsorbed species of methanol and water on the electrode surface.

In the case of methylformate, the production rate significantly increased with the increasing P_{CH_3OH}/P_{H_2O}. The plots were on a straight line with a slope of 2.07 in Fig. 8 showing that the production rate, y, was expressed by the power function of P_{CH_3OH}/P_{H_2O}, x, as $y = 329.8x^{2.07}$. The positive power function means that the production rate of that intermediate increased with the increasing of P_{CH_3OH}/P_{H_2O}. For formaldehyde, the production rate also increased with the increase in P_{CH_3OH}/P_{H_2O}, but with a weaker dependency. It was correlated by a power function of P_{CH_3OH}/P_{H_2O} having the power factor 0.47, $y = 38.3x^{0.47}$, as shown in Fig. 9. On the other hand, the production rate of formic acid decreased with the increasing P_{CH_3OH}/P_{H_2O} as shown in Fig. 10, showing a negative slope, in which the production rate was correlated by a power function of P_{CH_3OH}/P_{H_2O} having the power factor −0.57, $y = 4.5x^{-0.57}$.

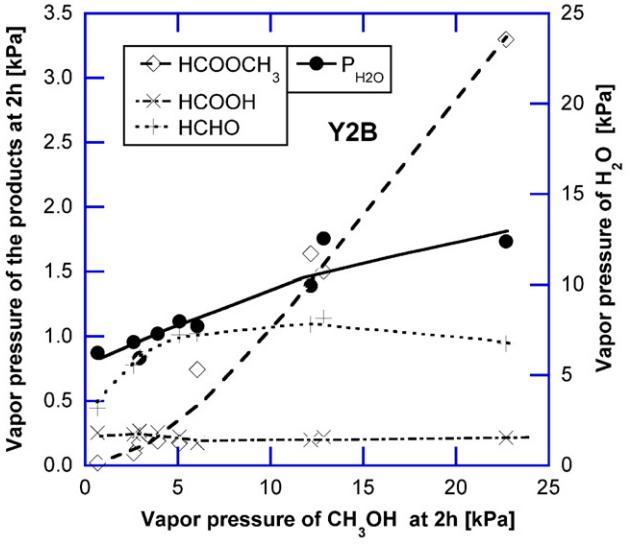

Fig. 7. Vapor pressure of intermediate products and P_{H_2O} in the anode gas layer at various of P_{CH_3OH} at 2 h operation.

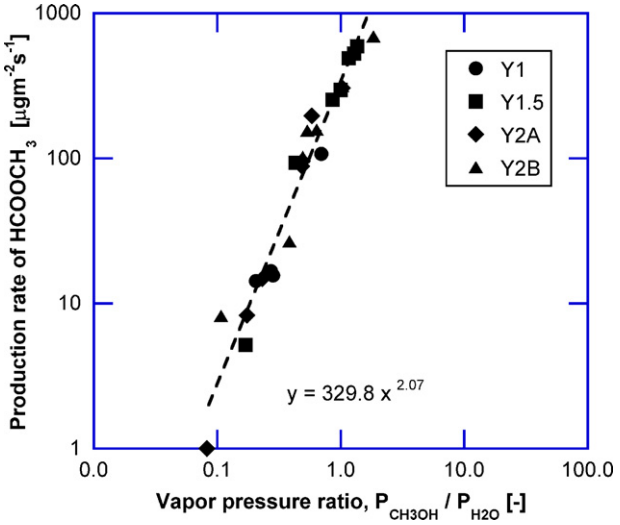

Fig. 8. Production rate of methyformate at various activities of P_{CH_3OH}/P_{H_2O}.

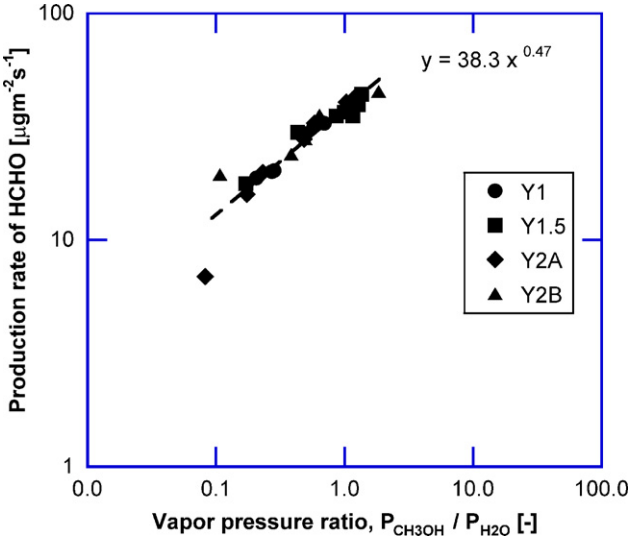

Fig. 9. Production rate of formaldehyde at various activities of P_{CH_3OH}/P_{H_2O}.

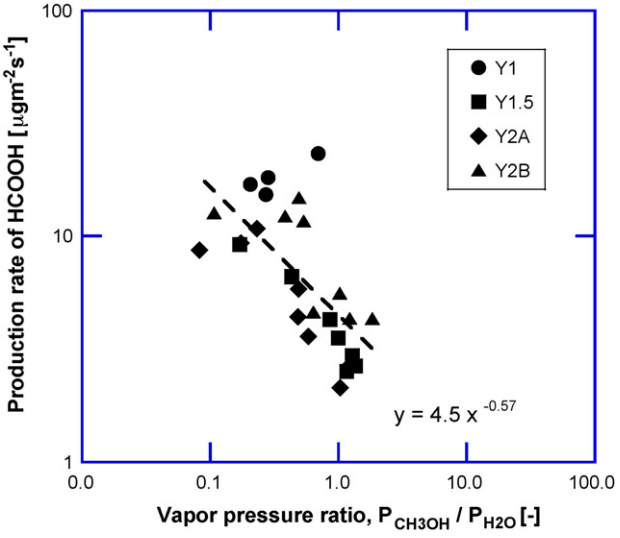

Fig. 10. Production rate of formic acid at various activities of P_{CH_3OH}/P_{H_2O}.

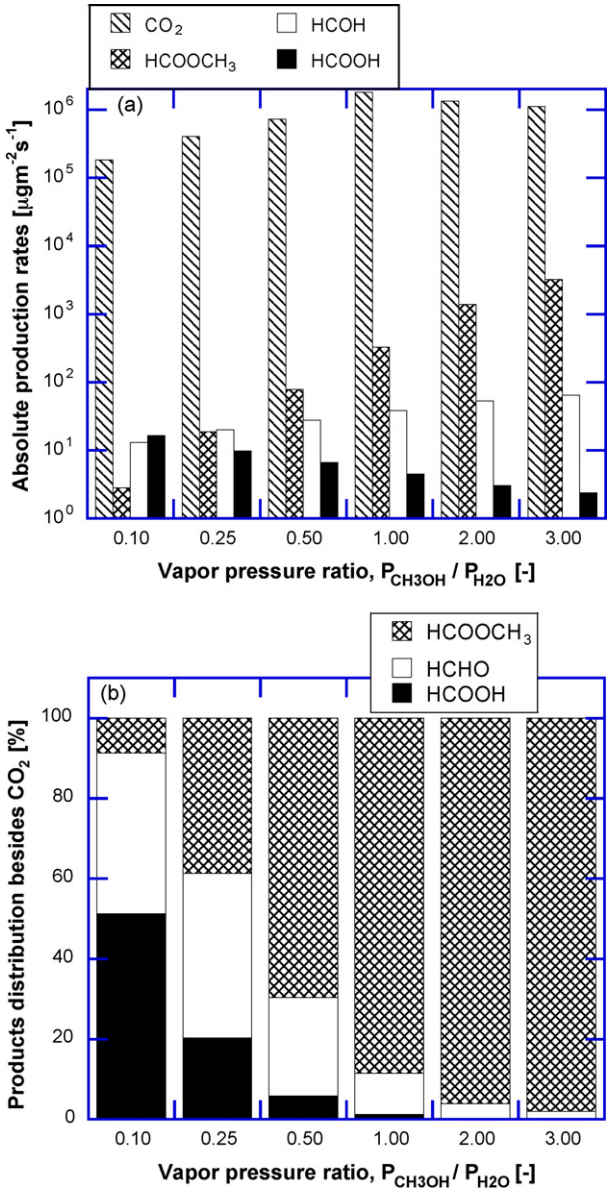

Fig. 11. Calculated products at various activities of P_{CH_3OH}/P_{H_2O}. (a) Absolute production rates including CO_2 and (b) products distribution besides CO_2.

Using the equations obtained from Figs. 8–10, we can calculate the production rate of each intermediate under the stated conditions of this study. The production rates of methylformate and formaldehyde at $P_{CH_3OH}/P_{H_2O} = 3.0$ were calculated to be 3196 $\mu g\,m^{-2}\,s^{-1}$ and 64 $\mu g\,m^{-2}\,s^{-1}$, respectively, which were more than 4 times less compared to those for methylformate and formaldehyde, 14451 $\mu g\,m^{-2}\,s^{-1}$ and 289 $\mu g\,m^{-2}\,s^{-1}$, respectively, obtained using a Pd black catalyst and phosphoric acid (H_3PO_4) electrolyte membrane [26]. The difference in the production rates between these two cases would be related to the difference in the catalyst and electrolyte.

Fig. 11 shows the calculated absolute production rate of the reaction products including CO_2, (a), and the calculated product distributions besides CO_2, (b), for different conditions of P_{CH_3OH}/P_{H_2O} at 2 h based on the production rates obtained from Figs. 8–10. For the calculation, it was assumed that no product initially existed and the compositions of these intermediates after a certain reaction time were estimated by integrating the obtained production rates. From Fig. 11(a), it was clearly shown that the production rate of CO_2

was higher in the range of 1.0E+3 to 1.0E+4 times compared to that of the other reaction products for all P_{CH_3OH}/P_{H_2O} and increased with the increasing of P_{CH_3OH}/P_{H_2O} up to $P_{CH_3OH}/P_{H_2O} = 1.0$. In the cases of methylformate and formaldehyde, one can easily understand that the production rates also have a tendency to increase with the increasing P_{CH_3OH}/P_{H_2O} while that of formic acid decreased with the ratio as following the equations obtained from Figs. 8–10.

A similar tendency for methyformate was shown in Fig. 11(b) for product distributions besides CO_2. At a very low partial pressure ratio like $P_{CH_3OH}/P_{H_2O} = 0.1$, the distribution showed the high selectivity for formic acid and formaldehyde of 51% and 40%, respectively, besides CO_2. These percentages decreased with the increasing P_{CH_3OH}/P_{H_2O}, while that of methylformate increased with the increasing ratio and reached 98%, besides CO_2, at $P_{CH_3OH}/P_{H_2O} = 3$. The calculated distribution qualitatively agreed with the previous study [27] that showed a high selectivity of 75%, besides CO_2, of formaldehyde at the low methanol vapor pressure, $P_{CH_3OH} = 1.0$ kPa, while methylformate with a high selectivity, 80%, besides CO_2, at a high vapor pressure of methanol, $P_{CH_3OH} = 12.9$ kPa. By measuring the gas composition in the gas layer using in situ mass spectrometry, the production rate of the intermediate was formulated as a function of the methanol and water vapor pressure ratio, P_{CH_3OH}/P_{H_2O}, and hence, the product distribution could be quantitatively estimated.

Meanwhile, in case of the production rate of CO_2 with respect to the electrical coulombs, the selectivity of the total intermediates from the converted methanol was calculated to be less than 0.5% even when the production rate of the methylformate reached 800 $\mu g\, m^{-2}\, s^{-1}$ at $P_{CH_3OH}/P_{H_2O} = 1.8$ in this study. Even, at a high ratio of vapor pressure, P_{CH_3OH}/P_{H_2O}, such as 3, the estimation of the total production rate of intermediates was also less than 1.0%. Hence, we can say that the energy loss by the intermediate products for the DMFC with PCP was negligibly small. We do not need to pay attention to the energy loss by the production of the intermediates as long as the vapor pressure ratio is controlled within a certain low level, like $P_{CH_3OH}/P_{H_2O} = 1$.

4. Conclusion

In situ mass spectrometry using a capillary probe was carried out in order to evaluate the production of the intermediate products of the anode gas layer of a semi-passive direct methanol fuel cell (DMFC) employing a porous carbon plate (PCP). Methylformate, formaldehyde, and formic acid were detected, and the profiles of their vapor pressures were measured. The production rates of these intermediates were related to the vapor pressure of methanol and water in the gas layer. The production rate of each intermediate was formulated as a power function of the methanol and water vapor pressure ratio, P_{CH_3OH}/P_{H_2O} with the power factor of 2.07, 0.47 and −0.57 for methylformate, formaldehyde, and formic acid, respectively. Based on these equations for the production rates, the product distribution could be quantitatively estimated.

Acknowledgements

A part of this study was supported by JSPS KAKENHI (1936057). The authors thank Mitsubishi Pencil Co. Ltd., for the gift of the porous carbon plate.

References

[1] B. Kho, I. Oh, S. Hong, H.Y. Ha, Electrochim. Acta 50 (2004) 781–785.
[2] T. Shimizu, T. Momma, M. Mohamedi, T. Osaka, S. Sarangapani, J. Power Sources 137 (2004) 277–283.
[3] D. Kim, E.A. Cho, S.A. Hong, I.H. Oh, H.Y. Ha, J. Power Sources 130 (2004) 172–177.
[4] Q. Ye, T.S. Zhao, J. Power Sources 147 (2005) 196–202.
[5] H. Qiao, M. Kunimatsu, T. Okada, J. Power Sources 139 (2005) 30–34.
[6] S.C. Thomas, X. Ren, S. Gottesfeld, P. Zelenay, Electrochim. Acta 47 (2002) 3741–3748.
[7] Q. Ye, T.S. Zhao, J. Electrochem. Soc. 152 (2005) A2238–A2245.
[8] Z.X. Liang, T.S. Zhao, J. Prabhuram, J. Membr. Sci. 283 (2006) 219–224.
[9] M.Y. Lo, I.H. Liao, C.C. Huang, Int. J. Hydrogen Energy 32 (2007) 731–735.
[10] I. Mizutani, Y. Liu, S. Mitsushima, K. Ota, N. Kamiya, J. Power Sources 156 (2006) 183–189.
[11] S. Surampudi, S.R. Narayanan, E. Vamos, H. Frank, G. Halpert, A.L. Conti, J. Kosek, G.K.S. Prakash, G.A. Olah, J. Power Sources 47 (1994) 377–385.
[12] M.K. Ravikumar, A.K. Shukla, J. Electrochem. Soc. 143 (1996) 2601–2606.
[13] S.R. Yoon, G.H. Hwang, W.I. Cho, I.H. Oh, S.A. Hong, H.Y. Ha, J. Power Sources 106 (2002) 215–223.
[14] R. Chen, T.S. Zhao, J. Power Sources 152 (2005) 122–130.
[15] B. Bae, B.K. Kho, T. Lim, I.H. Oh, S.A. Hong, H.Y. Ha, J. Power Sources 158 (2006) 1256–1261.
[16] N. Nakagawa, M.A. Abdelkareem, K. Sekimoto, J. Power Sources 160 (2006) 105–115.
[17] M.A. Abdelkareem, N. Nakagawa, J. Power Sources 162 (2006) 114–123.
[18] M.A. Abdelkareem, N. Nakagawa, J. Power Sources 165 (2007) 685–691.
[19] M.A. Abdelkareem, N. Morohashi, N. Nakagawa, J. Power Sources 172 (2007) 659–665.
[20] N. Nakagawa, K. Sekimoto, M.S. Masdar, R. Noda, J. Power Sources 186 (2009) 45–51.
[21] Y. Xiu, K. Kamata, N. Nakagawa, Electrochemistry 70 (2002) 946–949.
[22] I. Tkach, A. Panchenko, T. Kaz, V. Gogel, K.A. Friedrich, E. Roduner, J. Chem. Phys. 6 (2006) 5419–5426.
[23] C.A. Angelucci, L.J. Deiner, F.C. Nart, J. Solid State Electrochem. 12 (2008) 1599–1603.
[24] K. Otsuka, T. Ina, I. Yamanaka, Appl. Catal. 247 (2003) 219–229.
[25] H. Nakajima, H. Kita, Electrochim. Acta 33 (1992) 521–526.
[26] I. Yamanaka, K. Otsuka, Electrochim. Acta 34 (1989) 211–214.
[27] R. Liu, P.S. Fedkiw, J. Electrochem. Soc. 142 (1995) 3514–3523.
[28] T. Iwashita, Electrochim. Acta 47 (2002) 3663–3674.
[29] H. Wang, T. Loffler, H. Baltruschat, J. Appl. Electrochem. 31 (2001) 759–765.
[30] S. Wasmus, J.T. Wang, R.F. Savinell, J. Electrochem. Soc. 142 (1995) 3825–3833.
[31] I.T. Bae, J. Electrochem. Soc. 153 (2006) A2091–A2097.
[32] T. Nash, J. Biochem. 55 (1953) 416–421.
[33] http://webbook.nist.gov/chemistry/name-ser.html.